

TRANSVERSE COMPRESSION BEHAVIOR OF WOOD IN SATURATED STEAM AT 150-170°C

*Frederick A. Kamke**†

Professor
Department of Wood Science and Engineering
Oregon State University
Corvallis, OR

Andreja Kutnar

Researcher
Primorska Institute for Natural Sciences and Technology
University of Primorska, 6000 Koper, Slovenia

(Received March 2010)

Abstract. The transverse compression behavior of wood in high temperature (150, 160, and 170°C) and saturated steam conditions was studied. The effect of the temperature on the stress–strain response, nonlinear strain function, and relative density change was examined by a modified Hooke’s law based on the load-compression behavior of flexible foams. The influence of environmental conditions during compression on the set recovery of the compression deformation was determined. It was found that temperature and moisture content affected the compression behavior of wood in saturated steam conditions. A small difference in moisture content of specimens compressed at 160 and 170°C caused approximately the same stress–strain and relative density curves with minimum temperature affect on the compression behavior. The compressive modulus of the wood and cell wall modulus were found to decrease with increasing temperature from 150 to 160°C with no change when increased to 170°C. The densification region was entered at notably lower stress levels at 160 and 170°C when compared with 150°C. The results established that temperature and moisture content did not affect the nonlinear strain function at strain levels lower than 0.63. Furthermore, it was found that the set recovery of compressive deformation decreased with increasing temperature of compression from 150 to 160°C. In addition, the results showed that compression at 160 and 170°C significantly lowered the equilibrium moisture content.

Keywords: Cell wall modulus, densification, wood modification, thermal treatment, set recovery.

INTRODUCTION

All cellular materials, including wood, exhibit similarities in mechanical behavior (Gibson and Ashby 1988). During transverse compression loading, a typical stress–strain curve of wood has three distinct regions corresponding to three different mechanisms of cell deformation (Bodig 1963, 1965; Kennedy 1968; Wolcott et al 1994; Uhmeier et al 1998; Tabarsa and Chui 2000; Reiterer and Stanzl-Tschegg 2001; Nairn 2006). The initial part of the stress–strain curve for wood is linear elastic, where the stress is directly proportional to strain and the cell walls experi-

ence elastic deformation. The second part is a “plastic” or collapse region, where the stress is relatively constant although strain increases rapidly (ie the wood continues to deform at nearly constant stress). A yield point is exhibited at the beginning of cellular collapse. After the plastic region, the stress increases sharply with strain, which is from densification of cell wall material after the majority of cell walls have collapsed. Cellular collapse occurs by elastic buckling, plastic yielding, or brittle crushing depending on test conditions and the nature of the cell wall material (Lenth and Kamke 1996b). The initiation of each region of compression behavior is a function of cell geometry. Relative density of a cellular material, defined as the ratio of the apparent density of the material to the real density of the

* Corresponding author: fred.kamke@oregonstate.edu
† SWST member

solid of which it is made (Ribeiro and Costa 2007), is a characteristic feature that significantly impacts compression behavior of cellular materials.

Unlike most synthetic foam materials, wood has additional structural features that influence compressive properties. In addition to density, Nairn (2006) noted that percentage of latewood material, ray volume, and loading direction impact compression behavior. Several researchers have reported that wood responds differently to radial and tangential compression because of its anisotropic nature (Kunesh 1961; Kennedy 1968; Bodig and Jayne 1982; Dinwoodie 2000; Tabarsa and Chui 2000; Reiterer and Stanzl-Tschegg 2001; Kärenlampi et al 2003; Wang and Cooper 2005; Placet et al 2007). In radial compression, earlywood primarily controls the elastic and plastic parts of the stress-strain response, while the final consolidation stage is dominated by the elastic deformation of latewood. In the tangential direction, the final compression stage begins after buckling of the latewood layer (Tabarsa and Chui 2000). The different compressibility of wood tissue affects the distribution of void areas and thus the density distributions and mechanical properties of compressed wood (Kamke and Casey 1988; Lenth and Kamke 1996a; Thoemen and Ruf 2008).

Hydrothermal treatment has a strong influence on the mechanical behavior of wood during compression/densification. Softening and degradation will occur depending on the conditions such as temperature, moisture, steam, and time (Wolcott et al 1990; Morsing 2000). An increase of temperature or moisture content decreases the compressive modulus of wood (Kunesh 1961; Hillis and Rozsa 1978; Sadoh 1981; Östberg et al 1990). At low temperatures and low moisture contents, wood exhibits glassy behavior that can be characterized as stiff and brittle. At high temperatures (before thermal decomposition) and high moisture contents, wood has rubbery behavior that can be characterized as compliant. Between these two regions, the transition phase, typically called the glass transition, occurs (Wolcott et al

1994). Densification of wood by compression requires that cell walls are in a rubbery phase to obtain the compression deformation by cell wall buckling without cell wall fractures (Kutnar et al 2009), which has a very important effect on the improved mechanical properties of densified wood (Blomberg and Persson 2004; Kutnar et al 2008). The compression behavior of wood at high temperature and a pressurized steam environment has not been extensively studied. Therefore, the aim of this article is to characterize the compressive behavior of wood in transverse compression in saturated steam from 150 to 170°C.

MODEL DEVELOPMENT

The behavior of wood in transverse compression was modeled using a theory of cellular materials. The characteristic shape of the stress-strain relationship of wood was modeled by applying a modified Hook's law (Dai and Steiner 1993; Wolcott et al 1994; Lang and Wolcott 1996; Dai 2001; Zhou et al 2009) in the following form:

$$\sigma = E \varphi(\varepsilon) \varepsilon \quad (1)$$

where σ is compressive stress, E is transverse compression Young's modulus of the cellular material, ε is compressive strain, and $\varphi(\varepsilon)$ is the dimensionless strain function. The strain function is assumed to be independent of the properties of the cell wall and depends only on the cellular structure (Wolcott 1989; Dai and Steiner 1993; Zhou et al 2009). Therefore, loading conditions, temperature, and moisture content should not influence the strain function and impact only Young's modulus of the cell wall material. The value of $\varphi(\varepsilon)$ is equal to unity for strains in the linear elastic range, starts to decrease and reaches a minimum when the cell wall totally collapses, and finally increases rapidly and approaches infinity during cell wall densification.

The structural theories developed for honeycomb and closed cell foams may be applied to determine $\varphi(\varepsilon)$ with the following equation (Wolcott 1989; Lang and Wolcott 1996):

$$\varphi(\varepsilon) = [(C_3/C_2)/\varepsilon] \left[\frac{(1 - \rho_r^{1/3})}{(1 - \rho_r(\varepsilon)^{1/3})} \right] \tag{2}$$

where ρ_r is initial relative density of wood, $\rho_r(\varepsilon)$ is relative density as a function of compression strain, C_2 is the linear elastic constant, and C_3 is the product of C_2 and yield strain (ε_y). A thorough development of Eq 2 was provided by Gibson and Ashby (1988).

Relative density is defined as the ratio of the density of the cellular material to the density of the cell wall material (assumed to be 1500 kg/m³). The changing relative density ($\rho_r[\varepsilon]$) can be computed from the relationship between the plastic strain and the expansion ratio as follows (Wolcott 1989; Lang and Wolcott 1996):

$$\rho_r(\varepsilon) = \rho_r [1 - \varepsilon_p + 2/3 \mu \varepsilon_p - \mu \varepsilon_p^2]^{-1} \tag{3}$$

where ε_p is plastic strain ($\varepsilon_p = \varepsilon - \varepsilon_y$) and μ is the expansion ratio defined as the ratio of lateral strain to compressive strain in the nonlinear stress-strain region.

E is related to the Young's modulus of the cell wall (E_{cw}) and the cellular geometry, as represented by the relative density, as follows (Wolcott 1989):

$$E = C_2 E_{cw} \rho_r^3 \tag{4}$$

This expression states that the Young's modulus of any wood species could be calculated as a function of the cell wall modulus and the relative density.

MATERIAL AND METHODS

Materials

The butt log from low-density hybrid poplar (*Populus deltoides* × *Populus trichocarpa*) from a plantation located in northeastern Oregon was selected. The logs were approximately 0.25 m dia and were from 11-yr-old trees. The wood was sawn into lumber (approximately 25 mm thick), air-dried, and planed into 10-mm thick strips. The strips were placed in an environmentally controlled room (20°C, 65% RH) until equilibrium moisture content was achieved. The

oven-dry method was used on matched specimens to determine the initial mean moisture content of 12%. The strips were then planed to reduce thickness to 6 mm (radial) and cut to a length and width of 100 mm (longitudinal) and 60 mm (tangential), respectively. Special care was taken to ensure that the specimens with an average oven-dry density of 380 kg/m³ were taken from the same growth ring of the log to minimize the influence of wood variability.

Compression Procedure

Transverse compression of wood under saturated steam conditions and three temperatures (150, 160, and 170°C) was performed in a custom-built pressurized vessel that was equipped with a heated hydraulic press (Fig 1). The cylindrical vessel was heated by an electrical jacket heater. Platen temperature was independently controlled using two electrical resistance heater rods in each platen. Steam was supplied by a dedicated boiler. Thermocouples monitored platen and steam temperatures. Steam pressure was monitored with a pressure transducer in addition to a mechanical gauge. Temperature and steam pressure was controlled ±3°C and ±0.03 MPa, respectively. Force on the specimen was measured by a load cell (Omegadyne Inc, Sunbury, OH, Model

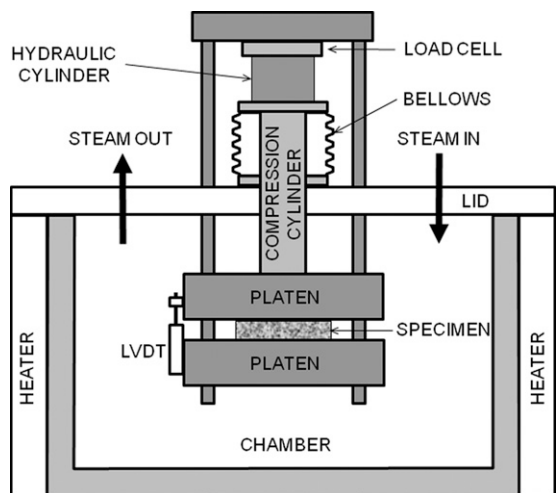


Figure 1. Schematic drawing of the pressure vessel used to compress specimens.

LC412-50K) that was located outside of the pressurized vessel. Force on the specimen was created using a hydraulic cylinder mounted outside of the vessel. Force was transferred from the hydraulic cylinder to the platens (180×180 mm) using a stainless steel compression cylinder that was sealed inside of a compressible bellows. The load cell was calibrated to account for steam pressure and mechanical resistance of the bellows. During compression, deformation was measured with a linear variable differential transformer (LVDT) connected to the heated platens of the press. The LVDT (Macro Sensors, Model HSTAR 750-500, ± 0.031 mm) was calibrated for temperature and steam pressure within the range of conditions used for this experiment.

Inside of the sealed vessel, the uncompressed specimens were first exposed to saturated steam for 3 min at the prescribed temperature followed by compression under saturated steam conditions at the loading rate of 1.3 MPa/min until 5.1 MPa was reached. The processes were completed with a final cooling stage to 100°C while the specimens were held under maximum compression stress. Cooling was accomplished by directing water through channels built into the platens. Cooling required 60-90 s depending on the treatment temperature. Ten replications were used for each treatment.

Before and after treatment, the specimen weight and dimensions were measured. After treatment, specimens were dried in a convection oven (103°C) overnight, oven-dry weight and dimensions were measured, and the mass loss, oven-dry density, and moisture content after compression were determined. The compressed specimens were placed into a controlled environment with 65% RH at 20°C until constant moisture content was achieved. After conditioning, the specimen moisture content was again determined and the density (ρ_{emc}), based on oven-dry weight, was calculated.

Set Recovery

To measure set recovery, specimens (50 mm longitudinal, 15 mm tangential) were cut from the

compressed wood specimens that were previously conditioned at 20°C and 65% RH. The remainder of the specimen was saved for future testing. Specimens were first dried in a convection oven overnight at 103°C , soaked in water for 24 h, dried again at 103°C , and final oven-dried thickness was recorded. The percentage of set recovery was determined by the following expression (Eq 5):

$$\text{Set recovery} = [(t_S - t_C)/(t_I - t_C)] \times 100[\%] \quad (5)$$

where t_S is oven-dry thickness after soaking, t_C oven-dry compressed thickness, and t_I initial uncompressed thickness.

All statistical analysis was performed using the multiple range test for significant difference with the 95% least significant difference procedure (Statgraphics 2000).

RESULTS AND DISCUSSION

Stress–Strain Response

Transverse compressive loading under saturated steam conditions at 150, 160, and 170°C followed a typical stress–strain curve of wood with three distinct regions corresponding to three different mechanisms of cell deformation (Fig 1). The linear elastic, collapse, and densification regions were each observed. Data from the linear elastic region of the stress–strain curve were used to determine the compression modulus of wood at each temperature. The compression modulus was obtained using a linear least square fit to the elastic portion of the curve (Table 1). The compression modulus of specimens compressed under saturated steam conditions at 150°C was 13 MPa. Increased temperature of compression to 160°C considerably decreased the compression modulus to only 5.9 MPa with only a slight change to 5.7 MPa with temperature increased to 170°C . The stress–strain response of wood at room temperature and 12% MC was measured and a compression modulus of 73 MPa was determined. Previous studies have reported that an increase of temperature or moisture content decreases the compressive modulus of wood (Kunesh 1961; Hillis and Rozsa 1978; Sadoh 1981; Östberg et al

1990). The results of this study are consistent with the consequence of the glass transition temperature (T_g), also known as the softening temperature. When the temperature of an amorphous polymer approaches T_g , the stiffness of the material decreases rapidly and continues to decline at a much slower pace in the rubbery phase. The stiffness is recoverable when the temperature is reduced. For wood above 20°C, the observed softening behavior has usually been attributed to lignin, although the amorphous component of cellulose has also been reported to contribute to this behavior. At saturated steam conditions of 150, 160, and 170°C, the wood material was above T_g and in the rubbery phase. The observed response of glass transition of wood occurs over a temperature range of approximately 50°C and is dependent on moisture content and the time domain of the observed mechanical response. T_g is typically reported in the literature as the midpoint of the

glass transition. In the time domain of 1-100 s, under water-saturated conditions, T_g of wood is approximately 70°C (Kelley et al 1987).

The average stress–strain curves presented in Fig 2 were used to determine the yield and densification stress and strain of the wood compressed at 150, 160, and 170°C (Table 1). Higher temperature of compression resulted in lower yield stress and lower densification stress. However, yield stress was approximately the same at 160 and 170°C. Furthermore, the yield and densification strains were found to be approximately the same regardless of the temperature of compression. The densification strain agrees with the 0.55 value reported by Wolcott (1989), while the yield strain was somewhat higher than the value of 0.03 expected for wood in this density range with an initial thickness of 6 mm. Note that Wolcott (1989) and Wolcott et al (1989) presented

Table 1. Yield and densification strain, yield and densification stress, and compression modulus of wood in transverse compression under saturated steam at 150, 160, and 170°C.^a

	Yield strain	Yield stress (MPa)	Densification strain	Densification stress (MPa)	Compression modulus (MPa)
150°C	0.059 (0.015)	1.1 (0.255)	0.56 (0.033)	2.3 (0.506)	13 (3.26)
160°C	0.053 (0.006)	0.57 (0.096)	0.57 (0.037)	1.6 (0.163)	5.9 (2.10)
170°C	0.058 (0.005)	0.66 (0.004)	0.56 (0.026)	1.3 (0.224)	5.7 (1.16)

^a Standard deviation shown in parentheses.

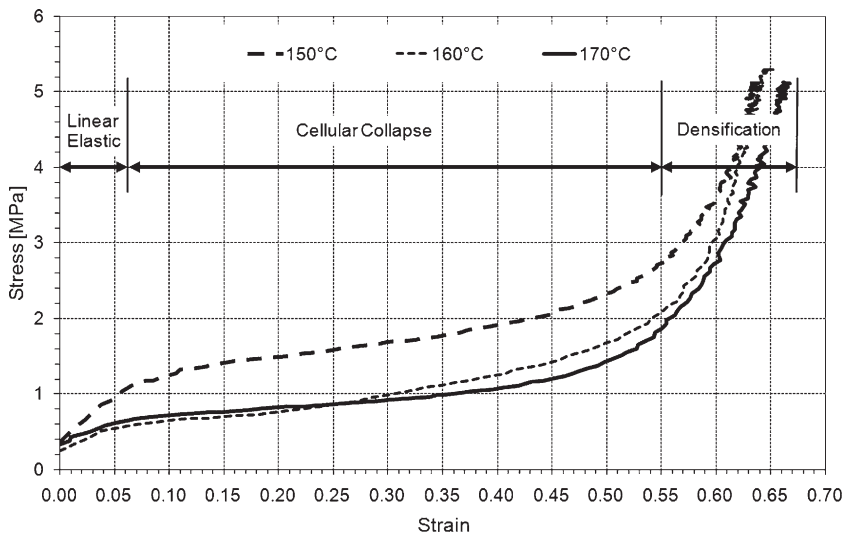


Figure 2. Average stress–strain curves of wood in transverse compression under saturated steam conditions at 150, 160, and 170°C.

an analysis of the effect of specimen height on compression behavior from restraint of the specimen surface in the compression apparatus.

Nonlinear Strain Function and Relative Density

The nonlinear strain function for each treatment was obtained from the average stress–strain response by Eq 2. Following Wolcott (1989), the value for linear elastic constant C_2 was assumed to be 0.57 for specimens of thickness equal to 6 mm, and the constant C_3 was determined as the product of C_2 and yield strain. The calculated nonlinear strain function of specimens compressed under saturated steam at 150, 160, and 170°C are plotted in Fig 3, in which each curve represents the average response of the replicates in each group. The curves are similar in magnitude and shape, and at strain of approximately 0.63, all curves overlapped. The results support the assumption made in previous studies (Wolcott et al 1990; Dai and Steiner 1993; Lang and Wolcott 1996; Lenth and Kamke 1996b) that the strain function is independent of temperature and moisture content. Zhou et al (2009) found that temperature and moisture affected the strain function at strains higher than 0.6 from chemical reactions of the wood poly-

mers that occur as the temperature approaches 200°C or at lower temperature in a high moisture environment. If any significant degradation occurred in the present experiment, the effect was apparently the same for each treatment. The higher final value of nonlinear strain function of specimens compressed at 160 and 170°C when compared with 150°C could be the consequence of thermal degradation reactions of some wood components during the compression process. Winandy and Krzysik (2007) reported no significant thermal degradation of aspen (*Populus* sp.) medium-density fiberboard fiber below 150°C, but loss of structural properties began after 200 s of exposure at temperature greater than 150°C.

The changing relative density ($\rho_r(\epsilon)$) was determined from the relationship between the plastic strain ϵ_p and the expansion ratio (μ) using Eq 3 (Fig 4). During transverse compression, the relative density increased as a result of the thickness reduction. The initial increase in relative density of specimens compressed at 160 and 170°C followed approximately the same curve, while at higher stress levels somewhat larger relative density was obtained in specimens compressed at 170°C. Furthermore, in specimens compressed at 150°C, higher stresses were required to reach the same change in relative

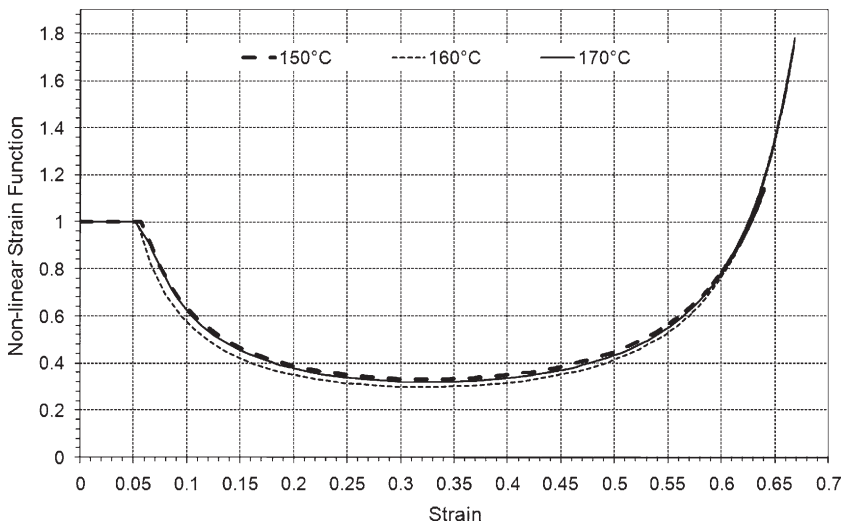


Figure 3. Nonlinear strain function $\phi(\epsilon)$ for wood in transverse compression under saturated steam conditions at 150, 160, and 170°C.

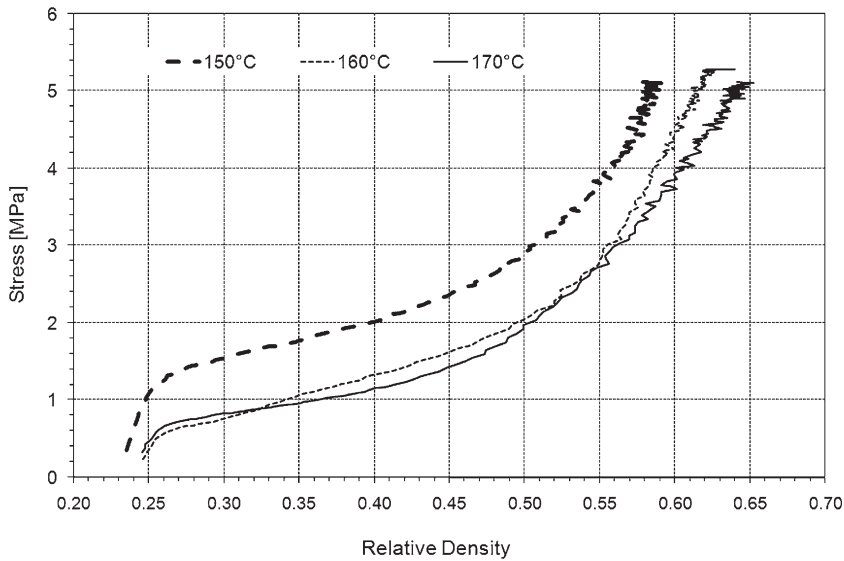


Figure 4. Relative density response of specimens compressed at constant rate of stress under saturated steam at 150, 160, and 170°C.

density over the entire compression range. The higher stress levels for specimens treated at 150°C are because of the higher compression modulus and higher yield stress for these specimens in comparison with the specimens compressed at 160 and 170°C.

It should be noted that in specimens compressed at 150°C, the expansion ratio (μ) was 0.026, which was considerably lower than the values of μ for specimens compressed at 160 and 170°C, which were 0.14 and 0.17, respectively (Table 2). The difference was from the significant difference in the width expansion between the specimens compressed at 150°C and those compressed at 160 and 170°C. Statistical analysis showed no significant difference between the two higher temperatures (Table 2). The strain measurement could have been influenced by swelling or shrinkage of the specimens from change of moisture content during the compression treatment. During compression, specimens could have gained moisture through the edges that were exposed to saturated steam, because the equilibrium moisture content inside the chamber was greater than the starting 12% MC. Adsorption of water would cause thickness

Table 2. Average ($n = 10$) thickness, width expansion, and expansion ratio for specimens immediately after compression under saturated steam at 150, 160, and 170°C.^a

Temperature (°C)	Compressed thickness (mm)	Width expansion (mm)	Expansion ratio (μ)
150	2.29 (0.166)	0.94 (0.47)	0.026
160	2.24 (0.160)	5.34 (1.55)	0.139
170	2.08 (0.274)	6.82 (3.24)	0.166

^a Standard deviation shown in parentheses.

swelling, which would have manifested in lower measured compressive deformation. No independent measurements were performed to isolate the influence of swelling and shrinkage of the specimens. Because only the edges of the specimens were exposed to the environment during compression, moisture content changes were likely small.

Cell Wall Modulus

The Young's modulus of the cell wall (E_{cw}) was determined using Eq 4 for each saturated steam condition. E_{cw} was affected by the temperature of compression. The highest E_{cw} of 1.4 GPa was found in specimens compressed at

150°C. Increased temperature of compression lowered E_{cw} at 160°C to 600 MPa and at 170°C to 580 MPa. There was no significant difference between the two higher temperature treatments. E_{cw} was approximately 100 times greater than the transverse compression modulus of the wood.

Zhou et al (2009) reported transverse compression modulus for aspen (*Populus* sp.) wood, at 80°C and 15% MC, to be 10 MPa, and at 110°C and 9% MC, to be 12 MPa. These conditions are both above T_g , and the relative density for aspen is about 0.25. The results by Zhou et al (2009) are close to the values reported in Table 1. Using Eq 4, the cell wall modulus of aspen would be 1.1 and 1.3 GPa for the conditions reported by Zhou et al (2009). Wolcott (1989) reported a calculated cell wall modulus for yellow-poplar (*Liriodendron tulipifera*) in saturated steam at 140°C of 16.7 GPa, which is higher than was expected, and 10 times greater than E_{cw} in the present study. Tabarsa (1999) reported E_{cw} for white spruce (*Picea glauca*) at 140°C and 6% MC to be 3.5 GPa. Tabarsa stated that cell wall modulus should be the same for all wood species. However, microfibril angle will affect E_{cw} , and T_g is known to vary between softwood and hardwood species. Xu and Liu (2004), using a theoretical micromechanics model, predicted cell wall modulus to change by a factor of 3 when microfibril angle changed from 40° to 10°. It must be noted that the hybrid poplar wood used in the present study was all tension wood, which contained a well-defined gelatinous (G) layer in the longitudinal fibers. One characteristic of the G layer is a low microfibril angle, which would contribute to a low transverse compression modulus. Comparison of E_{cw} values between different experiments can be done only if the same test

conditions (temperature, moisture content, and rate of load) are used; and then one must still consider differences in cell wall structure.

Properties of Compressed Wood

Oven-dry compressed density and moisture content of compressed specimens. The initial density was approximately the same for all specimens. After compression, the specimens were weighed, dried for 12 h in a convection oven at 103°C, and reweighed. Oven-dry compressed density values are shown in Table 3 and moisture content after compression is shown in Table 4. It had been assumed that 12 h was sufficient time to achieve a constant weight for the compressed specimens. The compression in saturated steam conditions caused some thermal degradation resulting in mass loss (Table 3). Higher temperature of the treatment led to greater mass loss, but the differences were not significantly different. The oven-dry density of the compressed specimens was to some extent influenced by the temperature of the compression. The highest oven-dry density after the treatment was obtained in the specimens compressed at 170°C. Statistical analysis showed that there was no significant difference in the oven-dry density of specimens compressed at 160 and 150°C, while oven-dry density of specimens compressed at 170°C was significantly higher. The determination of oven-dry density after conditioning in an environmental control room (20°C and 65% RH) showed an increase of oven-dry density. The measurement of specimen width after compression likely introduced some error in the density calculation. The compressed specimens sometimes had nonparallel edges immediately after processing. However, after conditioning, dimension measurements were

Table 3. Average ($n = 10$) mass loss and density of specimens before compression, immediately after compression, and after equilibration at 20°C and 65% RH.^a

	Initial oven-dry density (kg/m ³)	Mass loss (%)	Compressed oven-dry density (kg/m ³)	Compressed oven-dry density after conditioning (kg/m ³)
150°C	377 (16)	0.18 (0.705)	1070 (39)	1190 (60)
160°C	387 (28)	0.27 (0.396)	1070 (28)	1240 (85)
170°C	387 (37)	0.42 (0.612)	1110 (43)	1230 (94)

^a Standard deviation shown in parentheses.

Table 4. Average ($n = 10$) moisture content of the specimens before compression, after compression, and after conditioning in an environmental control room (20°C and 65% RH).^a

	Initial MC (%)	MC after treatment (%)	Equilibrium MC after compression in the environmental room (20°C, 65%) (%)
150°C	12	4.8 (2.3)	7.3 (0.72)
160°C	12	13 (2.2)	6.9 (0.82)
170°C	12	11 (3.7)	6.3 (0.47)

^a Standard deviation shown in parentheses. MC, moisture content.

performed on specimens that were cut and had a regular rectangular shape.

Table 4 shows the average moisture content of all treated specimens before compression, after compression, and after conditioning in an environmental controlled room (20°C and 65% RH). Before the compression treatment, all specimens had a moisture content of 12%. After the compression, the specimens compressed at 150 and 170°C had reduced moisture content, while the average moisture content of specimens compressed at 160°C was slightly increased. However, statistical analysis determined that the moisture content of specimens compressed at 160 and 170°C was not significantly different, while the moisture content of specimens compressed at 150°C was significantly lower. The results are suggesting that moisture content dominated the influence of temperature on the compressive behavior of wood. Low moisture content of specimens compressed at 150°C resulted in a different stress–strain curve and relative density change when compared with the curves of specimens compressed at 160 and 170°C. Small differences in moisture content of specimens compressed at 160 and 170°C caused approximately the same stress–strain and relative density curves with minimum temperature affect on the compression behavior.

Moisture content of compressed specimens was also determined after conditioning in an environmental control room (20°C, 65% RH). The temperature of the treatment affected moisture content after conditioning in the same manner as moisture content after the compression treatment. Higher temperature of the compression treatment

Table 5. Average ($n = 9$) thickness and set recovery of wood specimens compressed under saturated steam at 150, 160, and 170°C.^a

	Compressed oven-dry thickness (mm)	Oven-dry thickness after water soaking (mm)	Set recovery (%)
150°C	2.25 (0.184)	4.74 (0.298)	60.0 (11.9)
160°C	2.13 (0.151)	2.87 (0.464)	9.94 (6.29)
170°C	2.02 (0.236)	2.24 (0.137)	5.54 (6.24)

^a Standard deviation shown in parentheses.

resulted in lower moisture content after conditioning. Nevertheless, the moisture content of specimens compressed at 160 and 170°C did not significantly differ. The results were the consequence of temperature effect on equilibrium moisture content from thermal degradation expected in that temperature range. Lenth and Kamke (2001) reported equilibrium moisture content of approximately 7% for aspen wood at 160°C and 65% RH, which is very close to the results reported in Table 4. The previous study also noted 2% mass loss of xylan content after one complete desorption cycle (approximately 500 min exposure at 160°C as relative vapor pressure was reduced from 100 to 20%). Although the exposure conditions were different than the current study, it appears a reasonable expectation that some hemicelluloses were lost during the compression treatment, which resulted in lower hygroscopicity of the compressed specimens.

Set recovery. The temperature of compression under saturated steam conditions influenced the set recovery of the compressive deformation (Table 5). After the water soaking and drying cycle, the smallest set recovery was obtained in specimens compressed at 170°C. With decreased temperature of the compression set, recovery increased. However, there was no statistically significant difference in the set recovery between specimens compressed at 160 and 170°C, while the set recovery of specimens compressed at 150°C was significantly higher. The conditions of compression at 160 and 170°C under saturated steam minimized the buildup of internal stress and reduced hygroscopicity of the wood. The reduction of set recovery for wood compressed under saturated steam at high temperatures could be the result of a breakdown of the crosslinks

responsible for the memory effect in wood, perhaps a slight flow of lignin, or the formation of covalent bonds in the deformed position (Inoue et al 2008).

CONCLUSIONS

The transverse compression behavior of wood at temperatures of 150, 160, and 170°C under saturated steam environment was investigated. Based on a modified Hooke's law, the compressive stress was modeled as a function of elastic modulus of cell wall substance and a nonlinear strain function. For strain levels lower than 0.63, the results confirmed the assumption that the nonlinear strain function only depends on the cellular structure of the wood and is independent of temperature and moisture. At higher strains, differences in the nonlinear strain function were assumed to be the consequence of thermal degradation reactions of some wood components during the compression process. Furthermore, it was found that the temperature and moisture content affected the compression modulus of wood as a result of change of the cell wall modulus. In addition, compression under saturated steam conditions at 160 and 170°C considerably lowered the set recovery. The results of this study have significant importance for production of densified wood as well as hot-pressing of wood-based composites.

ACKNOWLEDGMENTS

The project was supported by the National Research Initiative of the USDA Cooperative State Research, Education and Extension Service, grant number 2006-35504-17444, and USDA Wood Utilization Research Center Special Grant number 2008-34158-19302.

REFERENCES

- Blomberg J, Persson B (2004) Plastic deformation in small clear pieces of Scots pine (*Pinus sylvestris*) during densification with the CaLignum process. *J Wood Sci* 50:307-314.
- Bodig J (1963) The peculiarity of compression of conifers in radial direction. *Forest Prod J* 13:438.
- Bodig J (1965) The effect of anatomy on the initial stress-strain relationship in transverse compression. *Forest Prod J* 15:197-202.
- Bodig J, Jayne BA (1982) *Mechanics of wood and wood composites*. Van Nostrand-Reinhold Co Inc, New York, NY. 711 pp.
- Dai C (2001) Viscoelasticity of wood composite mats during consolidation. *Wood Fiber Sci* 33(3):353-363.
- Dai C, Steiner PR (1993) Compression behavior of randomly formed wood flake mats. *Wood Fiber Sci* 25(4):349-358.
- Dinwoodie JM (2000) *Timber. Its nature and behavior*. BRE, London, UK, and New York, NY. 257 pp.
- Gibson LJ, Ashby MF (1988) *Cellular solids structure & properties*. Pergamon, New York, NY. 357 pp.
- Hillis WE, Rozsa AN (1978) The softening temperatures of wood. *Holzforschung* 32(2):68-73.
- Inoue M, Sekino N, Morooka T, Rowell RM, Norimoto M (2008) Fixation of compressive deformation in wood by pre-steaming. *J Trop For Sci* 20(4):273-281.
- Kamke FA, Casey LJ (1988) *Fundamentals of flakeboard manufacture: Internal-mat conditions*. *Forest Prod J* 38(6):38-44.
- Kärenlampi PP, Tynjälä P, Ström P (2003) Effect of temperature and compression on the mechanical behavior of steam-treated wood. *J Wood Sci* 49:298-304.
- Kelley SS, Rials TG, Glasser WG (1987) Relaxation behaviour of the amorphous components of wood. *J Mater Sci* 22:617-624.
- Kennedy RW (1968) Wood in transverse compression. *Forest Prod J* 18:36-40.
- Kunesh RH (1961) The inelastic behavior of wood: A new concept for improved panel forming processes. *Forest Prod J* 11:395-406.
- Kutnar A, Kamke FA, Sernek M (2008) The mechanical properties of densified VTC wood relevant for structural composites. *Holz Roh Werkst* 66(6):439-446.
- Kutnar A, Kamke FA, Sernek M (2009) Density profile and morphology of viscoelastic thermal compressed wood. *Wood Sci Technol* 43(1):57-68.
- Lang EM, Wolcott MP (1996) A model for viscoelastic consolidation of wood-strand mats. Part II: Static stress-strain behaviour of the mat. *Wood Fiber Sci* 28(3):369-379.
- Lenth CA, Kamke FA (1996a) Investigations of flakeboard mat consolidation. Part II. Modeling mat consolidation using theories of cellular materials. *Wood Fiber Sci* 28(3):309-319.
- Lenth CA, Kamke FA (1996b) Investigations of flakeboard mat consolidation. Part I. Characterizing the cellular structure. *Wood Fiber Sci* 28(2):153-167.
- Lenth CA, Kamke FA (2001) Equilibrium moisture content of wood in high-temperature pressurized environments. *Wood Fiber Sci* 33(1):104-118.
- Morsing N (2000) Densification of wood—The influence of hygrothermal treatment on compression of beech

- perpendicular to the grain. Department of Structural Engineering and Materials, Technical University of Denmark, Series R, 79. 138 pp.
- Nairn JA (2006) Numerical simulations of transverse compression and densification in wood. *Wood Fiber Sci* 38(4):576-591.
- Östberg G, Salmen L, Terlecki J (1990) Softening temperature of moist wood measured by differential calorimetry. *Holzforschung* 44:223-225.
- Placet V, Passard J, Perré P (2007) Viscoelastic properties of green wood across the grain measured by harmonic tests in the range 0-95°C: Hardwood vs. softwood and normal wood vs. reaction wood. *Holzforschung* 61:548-557.
- Reiterer A, Stanzl-Tschegg SE (2001) Compressive behavior of softwood under uniaxial loading at different orientations to the grain. *Mech Mater* 33:705-715.
- Ribeiro HA, Costa CAV (2007) Modeling and simulation of the nonlinear behavior of paper: A cellular materials approach. *Chem Eng Sci* 62:6696-6708.
- Sadov T (1981) Viscoelastic properties of wood in swelling systems. *Wood Sci Technol* 15:57-66.
- Statgraphics (2000) Statgraphics Plus version 5.0. Manugistics, Inc, Rockville, MD.
- Tabarsa T (1999) Compression perpendicular-to-grain behavior of wood. PhD Diss, The University of New Brunswick, Canada. 243 pp.
- Tabarsa T, Chui YH (2000) Stress-strain response of wood under radial compression. Part I. Test method and influences of cellular properties. *Wood Fiber Sci* 32(2): 144-152.
- Thoemen H, Ruf C (2008) Measuring and simulating the effects of the pressing schedule on the density profile development in wood-base composites. *Wood Fiber Sci* 40(3):325-338.
- Uhmeier A, Morooka T, Norimoto M (1998) Influence of thermal softening and degradation on radial compression behavior of wet spruce. *Holzforschung* 52(1):77-81.
- Wang JY, Cooper PA (2005) Effect of grain orientation and surface wetting on vertical density profiles of thermally compressed fir and spruce. *Holz Roh Werkst* 63:397-402.
- Winandy JE, Krzysik AM (2007) Thermal degradation of wood fibers during hot-pressing of MDF composites: Part I. Relative effects and benefits of thermal exposure. *Wood Fiber Sci* 39(3):450-461.
- Wolcott MP (1989) Modelling viscoelastic cellular materials for the pressing of wood composites. PhD Diss, Virginia Tech, Blacksburg, VA, 182 pp.
- Wolcott MP, Kamke FA, Dillard DA (1990) Fundamentals of flakeboard manufacture: viscoelastic behavior of the wood component. *Wood Fiber Sci* 22(4):345-361.
- Wolcott MP, Kamke FA, Dillard DA (1994) Fundamental aspects of wood deformation pertaining to manufacture of wood-base composites. *Wood Fiber Sci* 26(4):496-511.
- Wolcott MP, Kasal B, Kamke FA, Dillard DA (1989) Testing small wood specimens in transverse compression. *Wood Fiber Sci* 21(3):320-329.
- Xu P, Liu H (2004) Models of microfibril elastic modulus parallel to the cell axis. *Wood Sci Technol* 38:363-374.
- Zhou C, Smith GD, Dai C (2009) Characterizing hydrothermal compression behavior of aspen wood strands. *Holzforschung* 63:609-617.